Dvorak, Marc

An Alternative to the Born Rule : Spectral Quantization

Published in:
Foundations of Physics

DOI:
10.1007/s10701-023-00692-z

Published: 01/06/2023

Document Version
Publisher's PDF, also known as Version of record

Foundations of Physics (2023) 53:50
https://doi.org/10.1007/s10701-023-00692-z

An Alternative to the Born Rule: Spectral Quantization

Marc Dvorak[1]

Received: 15 May 2022 / Accepted: 21 April 2023

Abstract
We show that there is a hidden freedom in quantum many-body theory associated with overcompleteness of the time evolution through the single-particle subspace of a many-body system. To fix the freedom, an additional constraint is necessary. We argue that the appropriate constraint on the time evolution through the subspace is to quantize the propagation of entangled pairs of particles, represented by the single-particle spectral function, instead of individual particles. This solution method creates a surface that indicates the multiplicity of every solution to the inverse problem defined by matching the freedom to the constraint. Upon measurement, the system collapses nonlocally onto a single quantized solution. In addition to a combinatoric multiplicity, each solution acquires a multiplicity due to its stability when subject to a small variation in the microscopic degrees of freedom. Numerical calculations for a two-level system show that our theory improves upon standard theory in the description of non-quasiparticle spectral features. Our reinterpretation of quantum many-body theory is not based on the Born rule and offers a more faithful representation of experiments than current theory by modeling individual, quantized events with an explicit collapse model.

Keywords Quantum many-body theory · Entanglement · Quantum measurement · Wave function collapse · Non-Fermi liquid

1 Introduction

Nonrelativistic quantum many-body theory is a highly developed and extremely successful field. Nonetheless, theoretical challenges remain, and the one which motivates our study is a lack of consistency. Many-body theory takes place in Fock space, a much larger Hilbert space than for the noninteracting problem. The $N \pm 1$ portions of Fock space include excitations of the single-particle type, defined by

✉ Marc Dvorak
marc.dvorak@gmail.com

[1] Department of Applied Physics, Aalto University School of Science, 00076-Aalto Espoo, Finland

Published online: 05 May 2023

a single field operator acting on a reference configuration, and virtual excitations created by multiple field operators. Unitary time evolution of the many-body wave function covers all of Fock space, mixing both types of excitations, and is guaranteed to be norm conserving.

Effective field theories based on the single-particle Green's function, on the other hand, are built around a locally conserved current that passes through only the single-particle portion of Fock space. This single-particle basis is incomplete for the many-body problem. Even so, effective theories are constructed to have a normalized single-particle current, seemingly at odds with time evolution of the wave function through a much larger Fock space and the incompleteness of the single-particle basis.

Despite the advanced stage of the field, we do not consider the overall picture very clear. Our discussion raises a conceptual gap in many-body theory: how exactly does the many-body system propagate? At present, one can apparently choose between the two options discussed above: the high-dimensional wave function or a conserved current. Both of these objects are somehow normalized to the correct particle number despite their difference in dimensionality − an unsatisfying situation − and there is no clue about which one is physical or correct. Central to this question is the quantum measurement problem. At what point and how does the measurement condense the probability amplitude? What is the precise mechanism by which the probabilistic many-body state, an object much larger than can be observed, is reduced to a single, observable outcome? We want to close this gap in understanding.

Spectroscopies measure correlations between particles and are the primary means by which we gain information about quantum systems. The theoretical inconsistency discussed above can also be explained in the spectroscopic context. Experimental spectroscopies create and annihilate particles over some time interval, a process modeled theoretically with field operators. The field operators can act at any point in space and span the entire observable, three-dimensional space accessible in experiment. These operators represent the single-particle basis. Yet, the many-body system has some norm *beyond* this single-particle basis, even though any norm beyond the single-particle space cannot be measured.

The discrepancy between the quantum state and what can be measured arises because the wave function is a superposition of many-body configurations, and there are exponentially more configurations than there are single-particle states. What remains unclear to us is how to solve or completely understand this inconsistency.

There is a major hint at the mechanism behind a unified understanding of the single- and many-particle pictures: quantum entanglement. Indeed, we already know that correlations with the Schrödinger equation do not necessarily form a local current but can instead be entangled [1], with particles affecting each other nonlocally across indeterminate spacetime intervals. A complete and consistent theory of particle/hole correlations based on the Schrödinger equation should contain the entanglement effect.

Many aspects of nonlocality and entanglement are already understood by examining the entanglement structure of the many-body wave function. However, we want to develop a second-quantized formalism for entanglement. Such a field

theory-like description would, ideally, contain entanglement features of the wave function like nonlocal correlations and, at the same time, utilize the field operator formalism. Instead of being forced to choose between the wave function or a single-particle current, we want to combine features of both – a new theory with the entanglement structure of the full Schrödinger equation but in the language and reduced space of the single-particle Green's function.

In this article, we propose a solution to fully and consistently connect the single- and many-particle pictures. In brief, our idea is to quantize the correlation between particles instead of an individual particle. We show that there is a freedom in the quantum many-body problem that gives a choice of how to project the total correlation function into the single-particle subspace. To fix the freedom, we introduce a constraint on the resulting two-point equation, which is to quantize the creation, propagation, and annihilation of entangled particles *together*. Upon measurement, the many-body state collapses, and one such quantized solution is projected onto the single-particle, observable subspace. Counting these quantized solutions creates a multiplicity surface that can be compared with an experimental ensemble of spectroscopic measurements. We present numerical calculations for a two-level model system and discuss our concept in a broad context including comparisons with the single-particle Green's function, quasiparticles, and the reduced single-particle density matrix. Our proposal is a reinterpretation of the many-body wave function as a carrier of information about two-point, quantized correlations instead of a probability amplitude.

Our purpose in this article is to start building a theory that consistently and rigorously treats both the single- and many-particle pictures. We also want to understand the physical mechanism which enables transitions between the two. The scope of this manuscript is broad. We focus on general concepts in this initial exposition and not fine details.

2 Norm Conservation

We first give a clear demonstration of the problem we want to solve. We are interested in an isolated electronic system in equilibrium at zero temperature to which we can add or remove individual, quantized electrons. Our definition of norm or particle conservation is that for any initial single-particle creation/annihilation process, the total probability of annihilating/creating the added particle at any final time must be 1. This two-point normalization condition is necessary for the Green's function to make sense as a probability amplitude.

We are primarily concerned with the adiabatic, nonrelativistic electronic Hamiltonian of condensed matter [2, 3] and quantum chemistry [4],

$$\mathcal{H} = \sum_{ij} t_{ij}\, a_i^\dagger a_j + \frac{1}{2} \sum_{ijkl} v_{ijkl}\, a_i^\dagger a_j^\dagger a_l a_k, \tag{1}$$

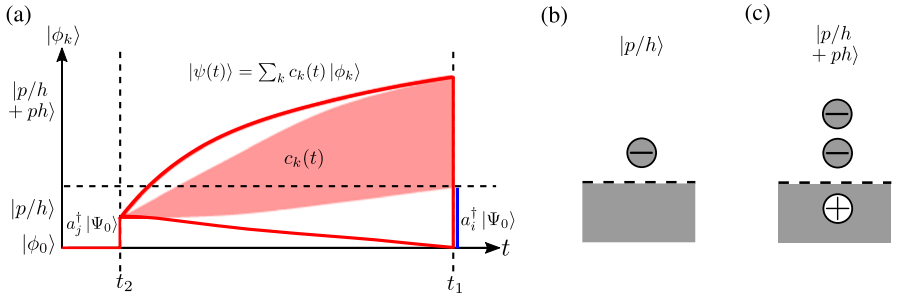

Fig. 1 (a) After an initial creation process, $a_j^\dagger|\Psi_0\rangle$, nonzero expansion coefficients $c_k(t)$ cover all of Fock space. At the final time, the overlaps with all possible annihilation processes recover the probability amplitude below the horizontal dashed line. The norm above the dashed line is on virtual excitations and not recoverable with G. The red outline shows the general case of how norm spreads across the full Fock space as the system evolves. The red shaded region depicts the specific and extreme case when all norm is transferred to virtual excitations, an excitation with zero quasiparticle residue. (b) and (c) show a particle (p/h) and particle plus particle-hole (p/h+ph) excitation, respectively. Excitations below the horizontal dashed line in (a) are of the type in (b), and excitations above the horizontal line in (a) are of the type in (c). The excitations in (b) and (c), which we refer to as particle and virtual, respectively, have the same particle number − one added electron

for one-body matrix elements t_{ij}, two-body matrix elements v_{ijkl}, and fermionic mode creation (annihilation) operators $a_i^\dagger$ (a_i). The single-particle Green's function in an orbital representation is [2, 3]

$$G_{ij}(t_1,t_2) = (-i)\frac{\langle\Psi_0|\hat{T}\,[\,a_i(t_1)\,a_j^\dagger(t_2)\,]\,|\Psi_0\rangle}{\langle\Psi_0|\Psi_0\rangle} \tag{2}$$

for interacting ground state $|\Psi_0\rangle$ and time-ordering operator $\hat{T}$. G describes the creation/annihilation of a particle at an initial time and the ensuing annihilation/creation of a particle at a final time.

The initial state in G is not an eigenstate of $\mathcal{H}$, in general. The repeated matrix multiplications from Taylor expanding the time evolution operator at internal times, $e^{\mp i\mathcal{H}(t_1-t_2)}$, mix all types of excitations in the $N \pm 1$ portion of Fock space. Fock space includes configurations with neutral particle-hole excitations attached to any added particle/hole. We label excitations with attached particle/hole pairs as virtual excitations. At any final time, the many-body state has nonzero expansion coefficients across the entire Fock space.

G is defined as the overlap at the final time with only the portion of these configurations with a single bare particle or hole. The total probability recoverable with G is found by summing over all possible single-particle annihilation/creation processes (summing down the column of G at the final time). Because the particle addition state after time evolution is distributed across the *entire* Fock space, and all possible single-particle annihilation/creation processes cover only a small portion of Fock space, the total recoverable probability is < 1. Only a fraction of a particle can be recovered by G at the final time. Simply put, the single-particle basis is incomplete.

This effect is demonstrated graphically in Fig. 1. For an initial particle creation on the ground state, which we assume is a single reference configuration $|\phi_0\rangle$, time evolution covers the entire Fock space. The expansion coefficients c_k for the configurations $|\phi_k\rangle$ are all nonzero, in general. The spread of norm to all c_k with time evolution is shown by the red outline in Fig. 1. At the final time, only the probability amplitude below the horizontal dashed line can be recovered with G, ruining the normalization of the final state in the single-particle subspace that is accessible in experiment.

It is even possible, in principle, that *all* of the norm is transferred to those configurations above the dashed line which have particle-hole pairs attached to the bare particle/hole (virtual excitations). This extreme case with all amplitude on virtual excitations is an excitation with zero quasiparticle residue, an outstanding challenge for theoretical physics, and shown by the red shaded region in Fig. 1.

Whether or not the lost norm is a problem and how to address it are additional issues. We argue that the norm lost to virtual excitations is a major problem. The intent of G is to describe the creation and ensuing annihilation of a normalized particle, exactly modeling a spectroscopy experiment. A possible solution to recover the lost norm is to somehow absorb the virtual excitations into renormalized field operators based on physical constraints. The theory can then be reconstructed or reinterpreted so that it respects the symmetries and conservation laws we impose.

For example, one can impose local continuity in the single-particle basis − a conserved single-particle current or probability density − in order to model a measured current. The result is that both initial and final states are normalized in the single-particle subspace. Such techniques, however, are the crux of the problematic inconsistency discussed thus far. We know that local time evolution of the many-body state covers *all* of Fock space, *not* just the single-particle portion.

As well-reasoned as it may be, local continuity is an external constraint on the many-particle theory. Based on *only* the Schrödinger equation, there is simply no reason for local continuity in the single-particle basis. In fact, both entanglement and the high-dimensional time evolution of the wave function suggest that this is actually not the case.

Our initial motivation is simple: recover the norm on virtual excitations that is part of the many-body wave function but lost in the definition of G. For this reason, we define a new correlation function, $\mathcal{G}$, that correlates all degrees of freedom in the $N \pm 1$ portions of Fock space. $\mathcal{G}$ has a Lehmann representation of

$$\mathcal{G}_{KK'}(\omega) = \sum_{N+1} \frac{\langle \Psi_0 | \Lambda_K | \Psi_{N+1} \rangle \langle \Psi_{N+1} | \Lambda_{K'}^\dagger | \Psi_0 \rangle}{\omega - (E_{N+1} - E_0) + i\eta} + \sum_{N-1} \frac{\langle \Psi_0 | \Lambda_{K'}^\dagger | \Psi_{N-1} \rangle \langle \Psi_{N-1} | \Lambda_K | \Psi_0 \rangle}{\omega - (E_0 - E_{N-1}) - i\eta}$$

where η is a positive infinitesimal. The operators Λ_K, $\Lambda_{K'}^\dagger$ create every possible excitation in the $N \pm 1$ portions of Fock space. Each Λ_K is a string of many single-particle field operators. For example,

$$\Lambda_K^\dagger = a_i^\dagger \tag{3}$$

$$\Lambda_K^\dagger = a_i^\dagger a_j a_k^\dagger \tag{4}$$

$$\Lambda_K^\dagger = a_i^\dagger a_j a_k^\dagger a_m a_n^\dagger \tag{5}$$

$$\ldots \tag{6}$$

where the composite index K includes all single-particle indices on the right-hand side. $|\Psi_{N+1}\rangle$ ($|\Psi_{N-1}\rangle$) are eigenstates of the $N+1$ ($N-1$) particle Hamiltonian with corresponding eigenvalues E_{N+1} (E_{N-1}). $|\Psi_0\rangle$ is the interacting ground state. We also refer to the $\Lambda_K^\dagger$ as composite excitations rather than virtual, since single-particle excitations of the type in Fig. 1b are allowed in the set of all K (as in Eq. 3). All of these excitations have the same particle number. $\mathcal{G}$ allows an initial state made from some number of field operators to decay into a final state with any other number of field operators (or the same number) that belongs to the sector of Fock space with the same particle number. $\mathcal{G}$ is extremely complicated, but can be defined quite simply as the largest possible time-ordered correlation function in the $N \pm 1$ portions of Fock space (the "total" correlation function).

As a starting point for a complete and consistent theory, $\mathcal{G}$ is an excellent choice. $\mathcal{G}$ contains all information about the total system and time evolution in the positions and residues of its poles. By summing down the column of $\mathcal{G}$ at the final time as in Fig. 1a, we can recover the full norm of the many-body state; no other correlation function can do this.

3 Spectral Layers

We eventually want to describe the addition/removal of normalized particles to the single-particle portion of the K, K' basis. To condense the total correlation function into the particle/hole subspace, we project $\mathcal{G}$ into the subspace of single-particle excitations.

Before detailing the exact projection of $\mathcal{G}$ onto the single-particle excitations, we demonstrate the key concept underlying our approach with an analogy. Consider a flashlight that illuminates a pencil in front of a screen. The shadow cast on the screen is the projection of the pencil. The three-dimensional pencil exists in a higher dimensional space than the two-dimensional screen. Accordingly, and *necessarily*, it is possible to rotate the pencil and find a new projection. This is purely a geometric effect, independent of any mathematical details of how the projection is performed. There is more information about the three-dimensional pencil than can fit on the two-dimensional screen. There are always more projections of the state (pencil)

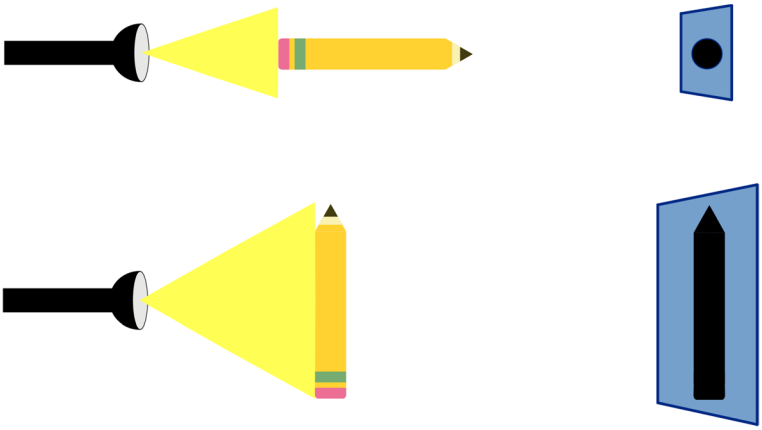

Fig. 2 When a flashlight illuminates a pencil, the projection of the pencil appears on the screen as a shadow. Because the pencil is higher dimensional than the screen, it can be rotated to have either a circular (top) or linear (bottom) projection. The screen is overcomplete with information about the pencil

than can fit in a subspace (screen). No matter which projection is selected, it always appears on the screen as two-dimensional (Fig. 2).

Our analogy is that the pencil represents the total correlation function $\mathcal{G}$. The screen is analogous to the single-particle subspace which can be measured experimentally. The projection of the pencil onto the screen by the flashlight represents the projection of $\mathcal{G}$ onto single-particle excitations. The screen can be considered overcomplete with projections of the pencil. That is, there are more projections of the pencil than can be shown on the screen at one time, a result of the dimensionality reduction from pencil to screen.

Despite its simplicity and without any equations, this simple example nicely demonstrates the core principle behind our idea: there is a fundamental freedom in choosing how to project the high-dimensional pencil ($\mathcal{G}$) onto the screen (single-particle subspace). Just as the screen is overcomplete with information about the pencil, the single-particle subspace is overcomplete with information about the many correlations contained in $\mathcal{G}$, as we now demonstrate.

Because we are interested in describing correlations between states, we must project different spectra contained in the total correlation function $\mathcal{G}$ onto the single-particle subspace. Spectra tell us the probabilities that one initial state decays into another and at which frequencies these decays can occur. The spectrum itself is defined by the imaginary part of the Green's function or correlation function of interest. We can simply take the imaginary part later and work directly with the correlation functions now.

To this end, we define projection amplitudes A_{iK} as

$$A_{iK} = \langle \Psi_0 | a_i \, \Lambda_K^\dagger | \Psi_0 \rangle \, . \tag{7}$$

A_{iK} projects the state $\Lambda_K^\dagger|\Psi_0\rangle$ defined by the composite excitation K onto the state $a_i^\dagger|\Psi_0\rangle$, a single-particle excitation. A_{iK} simply tells us how much of excitation i is in excitation K. The projection amplitude depends on states defined by excitations above the fully interacting ground state, a very complicated excitation process in the most general case. The ground state is not a single reference configuration with single-particle occupation numbers of 0 or 1. Consequently, these excitation processes are much more complicated than the case of working from a ground state that is a single reference configuration, either by assumption or after adiabatic connection from an interacting ground state [2]. We make no assumptions about the character of ground or excited states in our formalism.

We project every possible initial K excitation in $\mathcal{G}$ onto a single-particle excitation i; the same procedure is applied to final states K' by projecting onto single-particle excitation j. The resulting object, which we label the single-particle spectral projection matrix (abbreviated to projection matrix) and denote as $\overline{G}$, is

$$\overline{G}_{ij}(K,K',\omega) = A_{iK}\,\mathcal{G}_{KK'}(\omega)A_{K'j} \tag{8}$$

$$\begin{aligned}
=&\langle\Psi_0|a_i\,\Lambda_K^\dagger|\Psi_0\rangle\left(\sum_{N+1}\frac{\langle\Psi_0|\Lambda_K|\Psi_{N+1}\rangle\langle\Psi_{N+1}|\Lambda_{K'}^\dagger|\Psi_0\rangle}{\omega-(E_{N+1}-E_0)+i\eta}\right)\\
&\times\langle\Psi_0|\Lambda_{K'}a_j^\dagger|\Psi_0\rangle+\langle\Psi_0|\Lambda_{K'}^\dagger a_j|\Psi_0\rangle\\
&\times\left(\sum_{N-1}\frac{\langle\Psi_0|\Lambda_{K'}^\dagger|\Psi_{N-1}\rangle\langle\Psi_{N-1}|\Lambda_K|\Psi_0\rangle}{\omega-(E_0-E_{N-1})-i\eta}\right)\langle\Psi_0|a_i^\dagger\Lambda_K|\Psi_0\rangle\,.
\end{aligned} \tag{9}$$

Care must be taken in Eq. 9 to attach the proper particle or hole projection amplitudes A_{iK} to the corresponding particle or hole portion of $\mathcal{G}$.

Equation 9 is a complicated expression, but the meaning of $\overline{G}$ is straightforward. We compute a spectrum in the Lehmann representation for every possible creation/annihilation process, including offdiagonal ones, involving any number of field operators that create the correct particle number. We correlate all possible degrees of freedom. Then, every pair of initial and final excitations is projected onto the observable degrees of freedom − pairs of excitations defined by a single field operator. The projection has the same spectral shape as the original excitation pair but with a different normalization.

Again, we have carefully chosen to project onto the basis of states created by single field operators acting on the ground state. These operators represent the particles which can be measured in experiment. We consistently use i, j to denote single-particle excitations and K, K' to denote composite excitations. We remind the reader that all possible i are a subset of all possible K.

$\overline{G}$ depends on four independent indices: i, j, K, and K'. The projection of each pair of many-body excitations K and K' is therefore an entire matrix in the i, j basis. This again has a simple interpretation: an arbitrary excitation composed of any number of field operators (K or K') has some nonzero overlap with every possible single-particle excitation (i or j). The states created by these different

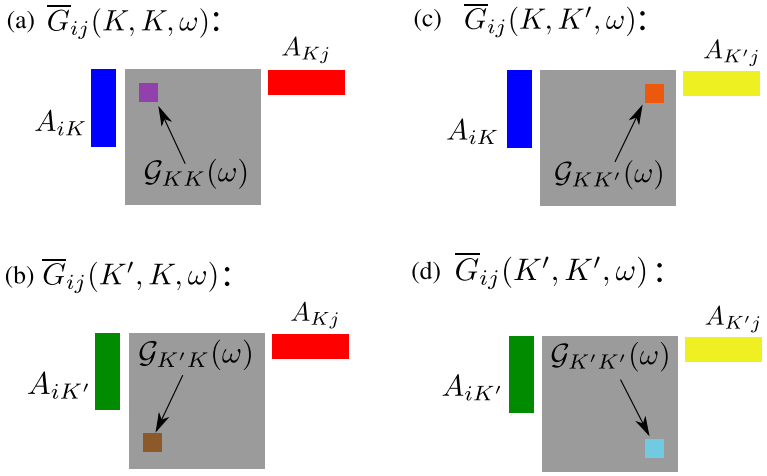

Fig. 3 Schematic of the matrix multiplications involved in $\overline{G}$. Each choice of K, K' is represented by a different position and color of the box in the grey square representing $\mathcal{G}$. For each choice, a vector and row of projection amplitudes are computed between the initial and final state of $\mathcal{G}$ (K or K') and all single-particle excitations. Their multiplication yields a matrix. K and K' run over a much larger set than i and j, hence the colored vectors and rows are shorter than the length of the grey square

excitations are, in general, not orthogonal. The projection amplitudes A_{iK} are therefore nonzero in the most general case and form a full matrix of amplitudes. The matrix multiplications involved in forming an entire i, j matrix for choice of K and K' are shown in Fig. 3.

i and j are fixed by the single-particle basis. These are the degrees of freedom which can be measured. K and K', however, are free parameters. There is a freedom in choosing K and K' in analogy with rotating the pencil in front of the screen to find a new projection. Because the space of all possible K is much larger than the space of all possible i, the projection of $\mathcal{G}$ onto $\overline{G}$ is not unique. Thus, K and K' in Eq. 9 represent a fundamental freedom in choosing how to project the total correlation function $\mathcal{G}$ onto the subspace of single-particle excitations. This projection freedom is an unavoidable consequence of the size and structure of the many-body problem; more specifically, of the reduction in dimensionality from full Hilbert space to subspace.[1]

In the Appendix (Sec. 8), we give yet another perspective on projecting information about the full system into a subspace based on the Löwdin downfolding technique for eigenstates. Our conclusion is the same: the hallmark of projecting or

[1] One could consider projecting only single-particle excitations i onto single-particle excitations j by the overlap A_{ij}. This case does technically provide a choice of which excitation to project *without* a reduction in dimensionality. This freedom is only due to the nonorthogonality of the states created by $a_i^\dagger$ and $a_j^\dagger$, however, and not what we have in mind. We consider this an "accidental" freedom. When projecting the full Hilbert space onto a subspace, the projection freedom is necessary and not accidental. The Appendix supports this view.

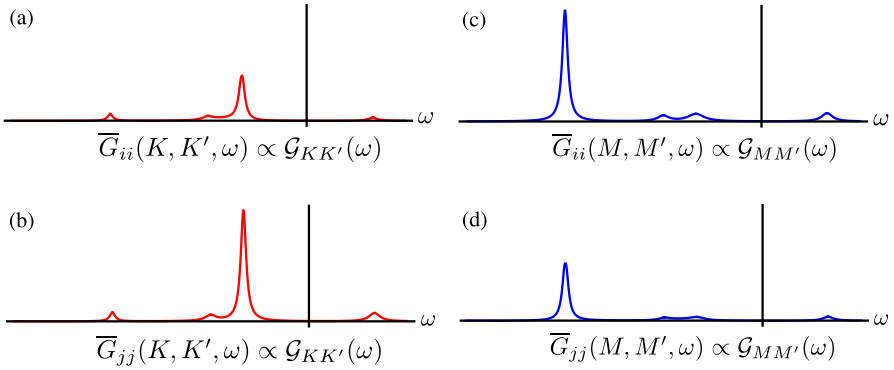

Fig. 4 A pair of composite excitations defined by a string of single-particle field operators (K, K' on the left, M, M' on the right) has its own spectrum in $\mathcal{G}$. The spectrum is related to the imaginary part of the correlation function. (a) and (b) have the same choice of composite excitation, as do (c) and (d). (a) and (b) have the same spectrum subject to different normalizations, as do (c) and (d). The choices K, K' or M, M' are different layers of the projection matrix $\overline{G}$

compressing information about the total system into a low-dimensional subspace is overcompleteness in the subspace or nonuniqueness of the projection.

At this point, K and K' are simply part of the definition of $\mathcal{G}$ and we leave them unspecified. Their selection is very important and will be discussed in detail in the next section.

The effect of projecting onto a subspace is to create "layers" to the spectrum of the projection matrix, as shown in Fig. 4. The subspace has many more spectra than it could normally support, leaving a choice of which spectrum to produce. The time evolution through the subspace is now overcomplete or nonunique, and there is a necessary free parameter, the K, K' pair, that allows us to choose the time evolution through the subspace.

The observable, single-particle spectrum in $\overline{G}$ changes with each choice of K, K'. A given matrix element holds many *spectral layers* of information. To an experimentalist who can only observe the single-particle subspace, each of these projections appears as a propagating particle, regardless of how many virtual particles would be attached to the full excitation.

In the limit of a single reference ground state and excited states made of a single Slater determinant, we recover in $\overline{G}$ the spectral function of G in the same limit. In this case, the amplitudes A_{iK} are zero for $i \neq K$ because states i and K are orthogonal. For weakly-correlated systems with little mixing of excitations, we expect the amplitudes A_{iK} to be very small for all excitations except the case $i = K$. In this case, we expect each spectral layer to be dominated by a quasiparticle solution. We expect very many of the matrix elements of $\overline{G}_{ij}$ to be nearly zero in most cases, at least for common electronic systems.

We are most interested, however, in understanding deviations from quasiparticle behavior in the strongly interacting limit. In this case, there could be significant offdiagonal amplitudes. This regime is explored numerically in our toy model in Sec. 6. In the direction of increasing correlation strength, the offdiagonal projection amplitudes

increase from zero (noninteracting limit), to small (weakly interacting), to large (strongly interacting).

Next, we next address the obvious question of how to choose K and K'. There is a fundamental freedom in choosing the layer or projection.

4 Collapse and Spectral Quantization

We assign the projection of $\mathcal{G}$ onto the single-particle basis meaning as the collapse of the many-body state upon measurement of the system. Originally, the system remains in a high-dimensional superposition of configurations across all of Fock space according to the Schrödinger equation. Then, it suddenly collapses with the measurement into the observable, single-particle subspace. We use the projection matrix as an explicit model for collapse of the wave function.

Our interpretation of the projection as collapse also guides our choice of which K, K' layer to project into the observable subspace. We see no *a priori* way to choose the layer onto which the system collapses. The choice of layer is extremely important, however, since it determines how the particle propagates.

To absorb the projection freedom, we need an additional constraint. The observed spectroscopic signal of the two-point process is always a normalized particle created at one point, propagating in time, and annihilated at another. This two-point creation/annihilation process is a correlation represented by a spectrum in the frequency domain – the same type of spectrum we have already been working with. However, unlike any given spectral layer of $\overline{G}$, the *observed* spectrum always has a very specific shape and normalization due to quantization. The normalized process is represented by a simple pole of residue 1 shifted off the real ω-axis by the physical broadening value $i\eta$. This shape means that the created/annihilated particles are normalized and the particle propagates with a definite frequency.

We use the projection freedom to *choose* the correlation that we observe. We search for linear combinations of the spectral layers that match the observed and normalized two-point signal. The final, observable event is a total projection assembled from different layers, each layer with its own weight. With measurement, the system collapses onto a quantized spectral projection.

Our strategy is to quantize the single-particle spectral function instead of a particle by itself. Since its discovery, entanglement has shown that the relevant and indivisible degree of freedom is the entangled pair, not the individual particles. Heuristically speaking, then, it makes sense to quantize a *pair* of particles instead of a single particle. Whether or not our idea can be formally connected to entanglement remains to be seen, but the physics of entanglement suggests such a two-point quantization is a credible approach.

Our quantization condition sets up a search through combinations of layers so that the single-particle spectral function of the total, observable projection, denoted M, is

$$\frac{1}{\pi} |\operatorname{Im} M_{ij}(\omega)| = \begin{cases} \delta_\eta(\omega - E_t), & i,j = x,y \\ 0, & \text{otherwise} \end{cases} \tag{10}$$

for some peak position E_t. We select a single matrix element in the single-particle excitation basis to quantize as a δ_η-function and set all other matrix elements to zero. The δ_η function in Eq. 10 represents our constraint and describes the creation, propagation, and annihilation of a single normalized particle, the most microscopic single-particle quantum mechanical process.

The structure of our proposed solution method, searching through an overcomplete space to find combinations of layers which match an observable signal, is an inverse problem. The total projection M is a sum of different layers of $\overline{G}$. We only need to consider the imaginary parts of the layers to match the quantization condition. We define spectral layer K, K' as $L_{ij}(K,K',\omega) = \operatorname{Im} \overline{G}_{ij}(K,K',\omega)$, the imaginary part of the single-particle spectral projection matrix. It depends on the free parameters K and K'. The inverse problem is to find the expansion coefficients $c_{KK'}$ for the layers which satisfy

$$\operatorname{Im} M_{ij} = \sum_{KK'} c_{KK'} L_{ij}(K,K',\omega) = \begin{cases} \pm\pi\, \delta_\eta(\omega - E_t), & i,j = x,y \\ 0, & \text{otherwise} \end{cases} \tag{11}$$

where we have quantized matrix element x, y in the single-particle excitation basis. Equation 11 constrains the free parameters K and K'. The $c_{KK'}$ select a quantized path that the particle can take through the system.

The observed process is one particle propagating from one state to another without any norm transferred to other states. For this reason, matrix elements of M_{ij} other than the one selected for quantization are set to zero. Our condition is therefore quantization on both the ω-axis (normalized δ_η-function) and in real space (zeroing other matrix elements $(i, j \neq x, y)$).

Equation 11 is a system of linear equations. We assume there is some number of solutions which match the quantization constraint at each x, y matrix element and frequency E_t with a multiplicity $W_{xy}(E_t)$. We make no restrictions on the layer coefficients $c_{KK'}$ and only require that the total projection is normalized. Normalization of the observed signal is what matters.

This sets up a very complicated problem for real systems. The idea is best explained graphically as in Fig. 5. Consider a single matrix element for two spectral layers of $\overline{G}$, one with a dominant peak at an energy E_1 and weak satellite at E_2, and the other with a strong peak at E_2 and a weak feature at E_1. Importantly, *neither* layer is quantized on its own. This is the behavior we expect for the exact layers of $\overline{G}$ and is due to the multiconfigurational character of the eigenstates.

To quantize the peak at E_1, we first give the E_1-dominated layer a weight so that the residue of that pole is 1. This also increases the amplitude on the weaker peak in that layer at E_2. To compensate, we add a contribution from the E_2-dominated layer with the sign and weight chosen so that it cancels the satellite peak in the first layer. Because the second layer is E_2 dominated, the numerical value of *its* satellite peak at E_1 is very small. We assume it does not ruin the normalization of the E_1 peak in the

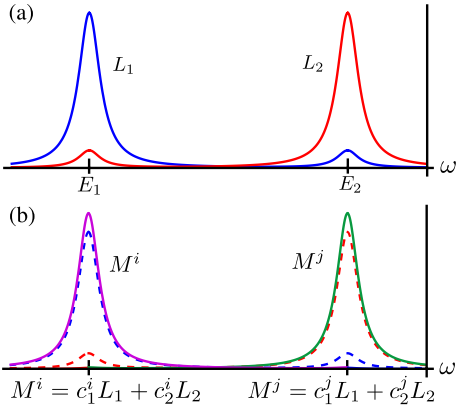

Fig. 5 Assume there are two layers of the single-particle spectral projection matrix L_1 and L_2. These layers have strong peaks at E_1 and E_2, respectively. The inverse problem of Eq. 11 searches for linear combinations of L_1 and L_2 to create quantized projections M_1 and M_2 The total, quantized projections, M_1 (purple) and M_2 (green), are linear combinations of L_1 and L_2. The expansion coefficients c are chosen to remove the extra features of the spectrum away from the main peaks. L_1 and L_2 are shown with dashed lines in (b) for comparison

first layer. Combined, these two layers form a quantized spectral projection within some numerical tolerance.

Identical arguments allow one to quantize the E_2 peak in the second layer with a small contribution from the other layer. The general idea is that for any weak feature of one spectral layer that ruins the quantization of the spectrum, there is a different layer in which that pole is the dominant peak and can be used to remove the weak feature in the first layer. We present numerical results corroborating this picture for a two-level model system in Sec. 6.

There is therefore a combinatoric effect which determines the multiplicity of each quantized solution. We expect the combinatoric multiplicity to be highest when quantizing peaks which are already strong in an individual layer. It is possible, in principle, that there are different combinations which give the same solution. Counting these different combinations defines the multiplicity, W, for that solution. Obviously, many combinations do not give quantized spectra and do not contribute to the multiplicity. Extremely weakly-correlated systems that lack satellite features in their spectra above a certain numerical tolerance could have quantized solutions composed of a single layer.

Until the measurement, the system remains in a high-dimensional superposition of configurations. Then, with collapse upon measurement, the initial and final states are both projected onto single-particle excitations. Our collapse model therefore has a nonlocal effect on the initial point. We interpret this as an actual, physical change to the system's history and initial configuration. Even the *choice* of the initial state is not determined until the collapse occurs, resulting in a nonlocal modification of the system's past. This is exactly the quantum entanglement effect we hoped to capture with a new theory for particle/hole correlations that remains consistent to the

Schrödinger equation. Our proposal is a two-point collapse, consistent with entanglement, instead of a single-point collapse onto the density.

Whether or not quantized solutions exist for a pair of points depends on the details of the Hamiltonian and any preparation of the initial many-body state, the structure of which requires exploration beyond the scope of this work. A formal connection to entanglement is desirable. If the Hamiltonian decouples into blocks, for example, one can speculate that there are no quantized solutions between states coming from different blocks. This could appear in the Lehmann amplitudes, which depend on the eigenstates, and/or through the projection amplitudes. $\overline{G}$ can be rewritten in a density matrix-like way, and our hope is that many properties of the reduced single-particle density matrix, including its entanglement structure, will carry over into our theory.

The expansion coefficients $c_{KK'}$ for each quantized spectrum are not related to normalization or probability amplitudes. They are just numbers which solve the inverse problem. Furthermore, by construction, each quantized spectrum is normalized. We cannot compare the residues of different events to each other – they are all 1. For these reasons, we need some other way to predict the probability of one collapse occurring over another. The *multiplicity* for each process holds that information. By comparing the multiplicities of different quantized processes to each other and/or summing over all processes to compute a total multiplicity, we can predict the probability of one collapse event occurring over any other. The total multiplicity is the normalization to convert the multiplicity surface to a probability distribution. Computing multiplicities is discussed more in the next section.

Finally, there is the normalization of the field operators. Because single-particle occupation numbers in the interacting ground state are not 0 or 1, the effect of a bare field operator on the interacting ground state is not to create a normalized particle. Our reintepretation remedies this issue. The projection matrix $\overline{G}$ is *defined* in the basis of states created by single field operators acting on the ground state. When we quantize matrix elements in this basis, the single, bare field operators behave exactly as we want (after the collapse of the system). By construction of our δ_η-function constraint on the inverse problem of Eq. 11, the bare field operators create/annihilate normalized particles above the interacting ground state.

5 Numerical Width

To continue developing our collapse model, we return to the analogy of projecting a pencil onto a screen. Consider the pencil and the flashlight. Within some numerical tolerance, very small rotations of the pencil give the same projection on the screen. As long as the rotation of the pencil causes a change to the projection which is less than the resolution of the screen, the resulting projection is the same to an observer of the screen. We can count each micro-rotation as a unique projection because it is distinct in the microscopic degrees of freedom. However, an observer will perceive a cluster of several of these small – though distinct – deviations around a single

projection as identical. This gives the observable projection on the screen a finite multiplicity.

There may be many ways to micro-rotate the pencil to reach the same projection on the screen, and we simply count them all to define the multiplicity of that projection. The observer or screen itself must have a finite resolution which is less than the resolution of the microscopic degrees of freedom, an idea built into our model, in order to be ignorant of these micro-rotations and give the macrostate (the projection on the screen) a finite number of microstates (micro-rotations of the same solution).

In order to generate a multiplicity with meaningful shape, it is essential to recognize that not all projections are equal. Instead of projecting a pencil, consider projecting a piece of paper. It is easy to project the broad side of the paper as a shadow on the screen. This projection is robust against slight deviations in the microscopic degrees of freedom. It is nearly impossible, however, to project the edge of the paper. Even though this projection technically exists, it takes incredible precision to actually create the projection. It is very unstable. These two projections are therefore unequal in terms of their robustness against microscopic deviations.

These examples demonstrate our concept of numerical width. To each projection, we attach a numerical width, or multiplicity, due to its (in)stability against small deviations in the microscopic degrees of freedom. More stable projections have a higher multiplicity.

Finite precision in the quantum system could potentially come from a number of sources including noise, stochastic fluctuations, etc., but we most strongly associate it with imprecise information about the positions of the electrons. If the screen has a finite resolution, for example, then the projection is insensitive to micro-rotations in the underlying degrees of freedom which induce a change less than the resolution of the screen. Without dwelling on the reason, we simply exclude infinitely precise projections from our model.

In principle, one should recompute the projection matrix for a cluster of small deviations in the microscopic parameters around a central point. We denote this abstract space of small deviations as a differential volume dV. At each perturbed set of coordinates inside of dV, one then solves the inverse problem for quantized projections. Counting solutions inside of dV contributes to the multiplicity through our concept of numerical width. This a separate effect contributing to W than the combinatorics of the inverse problem that we already discussed.

The previously outlined procedure is very expensive. We want a simpler procedure that renders the problem more tractable. Assume that, for a given quantized spectrum of interest, there is a certain contributing layer that is most sensitive to deviations in the microscopic degrees of freedom. Instead of solving the inverse problem at every point inside of dV, we can simply track how rapidly the projection amplitudes of that layer change as we move away from an optimal solution point inside of dV. Small changes to the amplitudes will make no difference and the combinatorics of the central point hold. However, a significant change can ruin the combinatorics required to reach the solution at the central point. Crudely speaking, the faster the amplitudes change away from a central point, the smaller the numerical width and multiplicity.

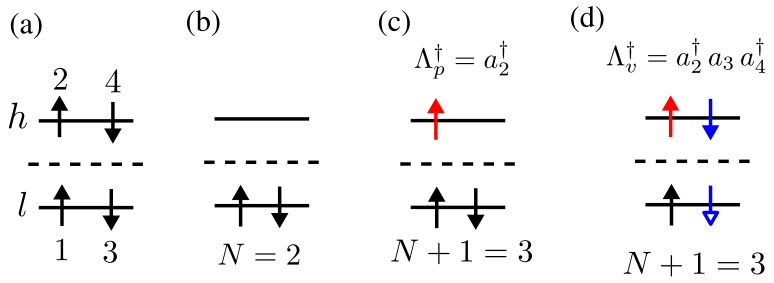

Fig. 6 Our two-level system has 4 spin-orbitals, shown in (a). The ground state in (b) has $N = 2$ electrons. We consider two excitations above the ground state: a particle excitation into state 2, shown in panel (c), and a composite excitation with an additional virtual particle-hole pair, shown in panel (d)

The relationship between the numerical width of a layer and the change in its projection amplitude is characterized by the equation

$$N_{ij}(K, K') = \left(\frac{\delta}{\delta \phi} A_{iK}\, A_{jK'} \right)^{-1} \tag{12}$$

where $N_{ij}(K, K')$ is the numerical width of matrix element i, j for layer K, K'. The variation $\delta/\delta\phi$ is an abstract representation of the change in the layer projection amplitudes due to some small perturbation ϕ. If the gradient is very large, the numerical width of the layer drops to zero. If the gradient is very small, the width of the layer increases. In this case, the change of the layer is very slow within the volume dV. This gives that layer a high multiplicity. Stationary points with respect to the variation $\delta/\delta\phi$ are especially noteworthy for their stability.

Our current equations are only approximate but convey the concept. These are not equations to compute the numerical widths in an absolute sense. They are, however, simple expressions which allow us to qualitatively capture the behavior we want. Exact equations for numerical widths are left to future work.

6 Two-Level Model

To demonstrate the virtues of our theory, we perform exact diagonalization (ED) calculations on a two-level model system. We use the eigenstates from ED to compute the Lehmann representation of $\mathcal{G}$, projection amplitudes A_{iK}, and spectral projection matrix. Our Hamiltonian is the interacting electronic Hamiltonian $\mathcal{H}$ of Eq. (1). Because of the number of overlap amplitudes involved in our formalism, an analytic result is cumbersome even for very simple systems. We instead resort to a numerical calculation.

Our two-level system is shown in Fig. 6. It contains two spatial levels, l (low) and h (high), each capable of holding two electrons in opposite spins. Spin dependent states are indexed from $1 - 4$. The ground state has $N = 2$ and particle addition connects to the $N + 1 = 3$ particle portion of the Hilbert space. In this sector, we limit

ourselves to particle addition only to state 2. There is a single spin-conserving virtual excitation in this sector, the creation of a particle in state 2 combined with the virtual particle-hole pair composed of states 4 and 3.

With these simplifications, the total correlation function $\mathcal{G}$ is only a 2×2 matrix. It contains one particle addition excitation into state 2 ($a_2^\dagger$), which we label $\Lambda_p^\dagger$, and one virtual excitation ($a_2^\dagger a_3 a_4^\dagger$), which we label $\Lambda_v^\dagger$. We emphasize that the simple depiction of the ground state and excitations in Fig. 6 is only for illustrative purposes. The true ground state is not a single Slater determinant with states 1 and 3 occupied; it is a superposition of many different configurations, a key component of our theory. The effects of the excitation operators $\Lambda_p^\dagger$ and $\Lambda_v^\dagger$ are therefore more complicated than what is shown in Fig. 6.

The advantage of these reductions is that $\overline{G}$ is a simple 1×1 matrix. Our entire single-particle basis is one state. We can therefore search for quantized spectra in just this matrix element without worrying about zeroing other matrix elements of $\overline{G}$. This matrix element of $\overline{G}$ has three layers corresponding to (creation, annihilation) excitations of (p, p), (p, v), and (v, v). These are the three unique matrix elements of the 2×2 matrix $\mathcal{G}$. Based on our previous discussion, we are especially interested in the transfer of norm from the excitation p to the excitation v and how it manifests itself in our theory. This is the norm lost to virtual excitations and unaccounted for in the single-particle G.

We make further simplifications in order to isolate the effects of interest. We consider only an on-site Coulomb interaction U (equivalent to Coulomb matrix elements v_{llll} or v_{hhhh}) and a direct interaction D (equivalent to Coulomb matrix element v_{lhlh}). The interesting physics relevant to our formalism is driven by offdiagonal matrix elements of the Hamiltonian. Offdiagonal elements are responsible for transferring norm from the particle space to the virtual space during time evolution. Neither U nor D contribute to the offdiagonal Hamiltonian. We instead parameterize the offdiagonal elements of H by the offdiagonal kinetic terms $t_{lh} = t_{hl}^*$. We vary t_{lh} to control the correlation strength in our model system.

Finally, we must compute the numerical width for each projection. For this, we employ a finite difference approach by repeating the calculation for a given set of parameters with a small increment added to t_{lh}, δt_{lh}. This small change in kinetic energy, δt_{lh}, represents some small deviation in the spatial coordinates of the electrons. We estimate the numerical width of the projection by selecting the most important layer and computing its change in amplitude with respect to the increment δt_{lh}. The numerical width is the inverse of this change, as in Eq. 12. This value is meaningless in an absolute sense but can be used to compare the stabilities of two different projections from the same ED calculation.

Figure 7 shows the single-particle spectral function $A(\omega) = |\mathrm{Im}\, G(\omega)|/\pi$, the spectra of the three unique matrix elements of $\mathcal{G}(\omega)$, our computed multiplicity, and the spectral layers L. The comparison between the vertically aligned panels (b) and (d) allows one to deduce the magnitude of the projection amplitudes A_{iK}. Corresponding matrix elements between (b) and (d) keep their spectral shape. The comparison tells how strongly each matrix element of $\mathcal{G}(\omega)$ is projected onto the basis of single-particle excitations. Panel (b) shows three separate *matrix elements* of $\mathcal{G}(\omega)$; panel (d) shows three different *layers* of a *single* matrix element.

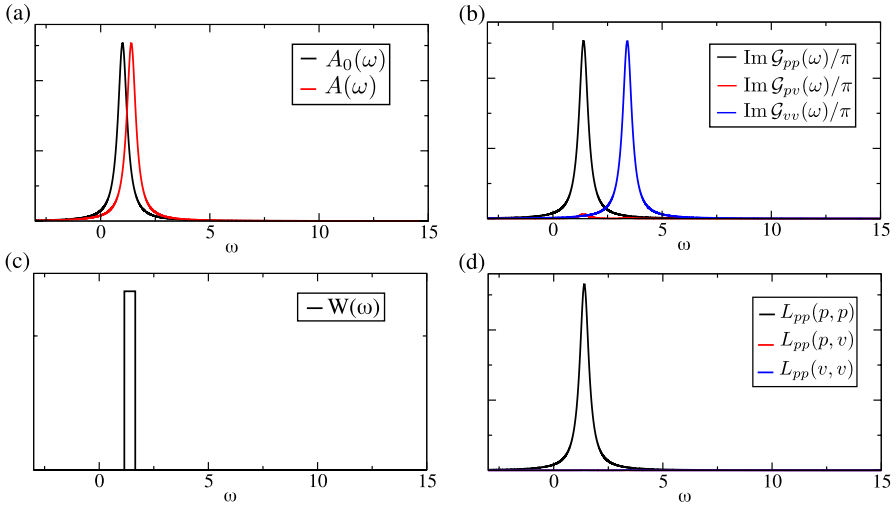

Fig. 7 (a) Spectral function of the noninteracting single-particle Green's function ($A_0(\omega)$) and interacting Green's function ($A(\omega)$) for a weakly-correlated two-level system. (b) Matrix elements of the total correlation function $\mathcal{G}(\omega)$. (c) Multiplicity of quantized projections. (d) Spectral layers in the single-particle basis. The scales for the vertical axes are arbitrary

The parameters in Fig. 7 are $U = 0.5$, $D = 0.2$, $t_{ll} = -1.0$, $t_{hh} = 1.0$, and $t_{lh} = 0.05$. This system is weakly correlated. The spectral function $A(\omega)$ in panel (a) nearly overlaps with the noninteracting spectrum $A_0(\omega)$. $\mathcal{G}_{pp}$ shows a single, clearly-defined peak at the first particle addition energy, and $\mathcal{G}_{vv}$ shows a single peak at the second excitation energy. There is little mixing of these excitations and, as a result, $\mathcal{G}_{pv}$ is weak. After projecting these matrix elements onto the state $\Lambda_p^\dagger|\Psi_0\rangle$, only the $\mathcal{G}_{pp}(\omega)$ layer survives. This is visible in panel (d). Consequently, there is a single peak in the multiplicity from the $L_{pp}(p,p)$ layer at the quasiparticle energy.

In this case, the multiplicity closely matches the spectral function of G. This is a good result. For weakly-correlated systems, we should recover the successful results of the single-particle Green's function. We do not want major numerical deviations from $A(\omega)$ for these systems. Because the offdiagonal projection amplitude A_{vp} is very small, we essentially just project the $\mathcal{G}_{pp}$ element, whose imaginary part is exactly the spectral function of G, onto the p, p matrix element of $\overline{G}$. This spectral layer shows no satellite features, trivially satisfies our quantization condition, and creates a peak in the multiplicity.

Turning up the correlation strength by raising t_{lh} to 0.4 in Fig. 8, we see that the offdiagonal matrix element $\mathcal{G}_{pv}$ is larger. This system has some norm transferred away from the particle excitation p onto the virtual excitation v. After projecting matrix elements of $\mathcal{G}$ onto the single matrix element of $\overline{G}$, all three layers have some amplitude. Even though the blue spectrum in Fig. 8d is very weak, it has the correct shape for quantization. It can be renormalized with the proper choice of expansion coefficient for that layer, c_{vv}, to create a properly quantized spectrum. In this case, c_{vv} must be relatively large, but the value of the expansion coefficient c_{vv} does not affect

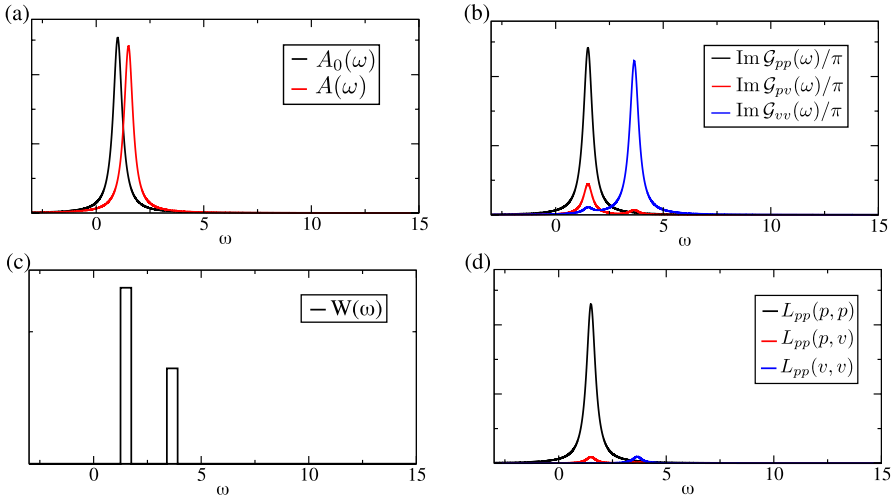

Fig. 8 Same as Fig. 7 but for medium correlation, $t_{lh} = 0.4$

the multiplicity. The $c_{KK'}$ are simply parameters in our theory to find quantized paths through the system.

The layer $L_{pp}(v, v)$ is less stable than $L_{pp}(p, p)$ according to our finite difference test with the increment δt_{lh}. The instability of layer $L_{pp}(v, v)$ creates a smaller peak in the multiplicity in panel Fig. 8c at higher energy. It is again an appealing result, for the sake of reproducing successful results of the single-particle G, that weakly projected layers (those with small A_{iK}) have greater instabilities and lower multiplicities. This mimics the overlap amplitude interpretation of the spectral function. It is not obvious or guaranteed that it should be this way, but we generally find this to be true for weak to moderate correlation.

A clear counterexample to this behavior, and the case we are most interested in, is the strongly-correlated example in Fig. 9. In this case, with $t_{lh} = 4.0$, there is strong mixing of excitations. Matrix elements of $\mathcal{G}$ all show meaningful spectra, and $\mathcal{G}_{vv}$ has peaks at both eigenvalues of the system. The offdiagonal projection amplitudes do not vanish and the layers all have some amplitude after projecting back into the particle subspace. To quantize the layer $L_{pp}(v, v)$, a contribution from either $L_{pp}(p, v)$ or $L_{pp}(p, p)$ with the opposite sign is necessary to remove the feature in $L_{pp}(v, v)$ at lower energy. This combination satisfies the inverse problem and gives a quantized spectrum at the higher eigenvalue. This quantized spectrum is an example of one with a combinatoric multiplicity greater than 1. $L_{pp}(p, v)$ and $L_{pp}(p, p)$ have essentially the same shape, and $L_{pp}(v, v)$ can be combined with either one to form a quantized solution.

In this case, the offdiagonal projection amplitude A_{vp} is actually *more stable* against small deviations in the microscopic degrees of freedom than the diagonal projection A_{pp}, *even though* A_{vp} is smaller. For this reason, the multiplicity has a larger peak at the higher energy solution. By comparison with $A(\omega)$, we see that this non-quasiparticle feature is entirely absent from the single-particle Green's function.

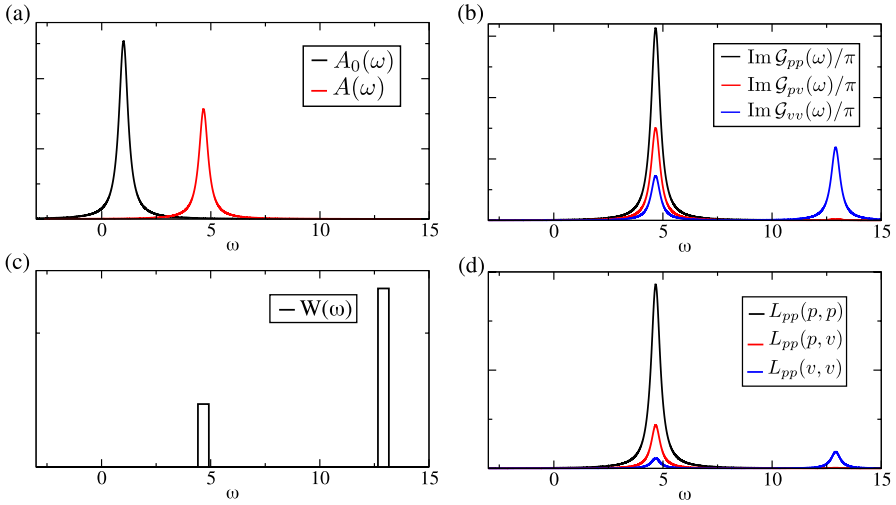

Fig. 9 Same as Fig. 7 but for $t_{th} = 4.0$. The data in panel (d) has been rescaled for better visualization. Different curves within panel (d) can still be compared to each other

By the nature of projecting the virtual excitation v onto the particle excitation p, it is a *non-quasiparticle* feature. It is only because the eigenstates are multiconfigurational (superposition of many different configurations) that there is a nonzero projection amplitude between the particle and virtual excitations. This distinctly quantum many-body behavior, in turn, is why we recover the non-quasiparticle feature.

The appearance of this additional peak in the multiplicity is a direct result of the norm transferred to virtual excitations. It is − *exactly* − the spectral projection of the virtual excitation. This is precisely the issue we wanted to address, and it leads to a very significant difference compared to the standard theory. We cannot overemphasize the potential impact of this difference from standard theory on the description of non-quasiparticle excitations.

7 Discussion

We now focus on the interpretation of our proposed reformulation, give perspective on its relation to current ideas, and the critical points that distinguish it from established theory.

Figure 10 shows the different steps in comparing an experimental ensemble of spectroscopic measurements to theory. Figure 10a shows a single measurement on a detector for a given process. One measurement always produces a normalized δ -function broadened by the physical value η. Panel (b) shows an ensemble of measurements. Each measurement produces its own ping on the detector at a certain frequency. In Fig. 10c, we have added the individual measurements of (b) together to form a histogram of the experimental data. The portion of Fig. 10 above the

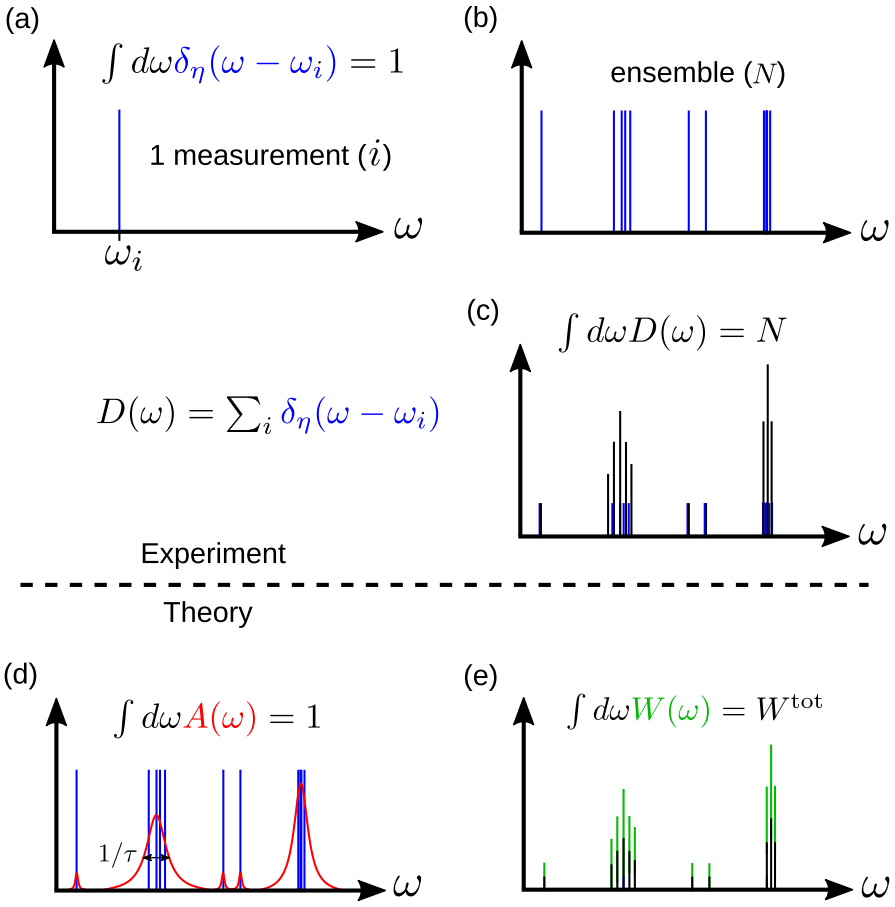

Fig. 10 Panels above the horizontal dashed line show the experimental process of measurement and building a histogram from the ensemble of N measurements. Panels below the horizontal line are theoretical comparisons to the experimental ensemble spectrum, labeled $D(\omega)$. Quasiparticle theory is illustrated in **d**; our own framework for generating the theoretical multiplicity is shown in **e**. Blue and black bars are drawn to scale throughout

horizontal dashed line is not meant for interpretation or discussion; it is simply a schematic of the process of collecting spectroscopic data.

Panels below the dashed line in the figure represent theoretical comparisons to the ensemble. Panel (d) shows the spectral function, $A(\omega)$, of the single-particle Green's function, G. $A(\omega)$ is normalized, and the size of a single measurement (blue bar) can be used as a consistent scale throughout Fig. 10. The common approach of many-body theory is to identify quasiparticles in panel (d) where the spectrum has clearly defined peaks. This is indicated by the lifetime width $1/\tau$ around the first main peak. The quasiparticle is then considered the relevant degree of freedom. In this quasiparticle description, what has happened is that the properties of an *ensemble* of

statistics are now being ascribed to a *single* object, the quasiparticle. It is only by measuring the ensemble that properties like the quasiparticle lifetime appear.

In practice, we measure infinitely sharp δ-functions, not quasiparticles, as shown in Figs. 10a and b. A single measurement never yields the spectrum of $A(\omega)$ or even shows a peak with an identifiable lifetime. We consider the quasiparticle-ization of the ensemble to be a conceptual leap to fit in the language and formalism of the single-particle Green's function. It is an extremely successful paradigm, but we do not consider this picture a faithful representation of the experiment.

Our new approach in Fig. 10e is different. The inverse problem of Sec. 4 describes the individual spectroscopic pings that appear on the detector. This theoretical process is a faithful representation of what is measured in experiment in panels (a) and (b). By abandoning the quasiparticle concept, our formulation also has a clear advantage: it is completely general and naturally describes systems without quasiparticles like non-Fermi liquids.

It is somewhat understood that quasiparticles are not fundamental degrees of freedom and argued that a more fundamental description is not necessary to describe what is observable. The assumption, at least as we understand it, is that the physical structure of the effective field theory is correct, even if observables must be renormalized. However, the structure of our formulation is completely different than an effective field theory. In our formulation, particles do not locally propagate from one spacetime point to another. Instead, the wave function collapses nonlocally. This difference in structure and foundational principles could lead to dramatically different physics.

Counting the ways that each process can be realized builds up the multiplicity, W, which can be compared to the experimental ensemble. W is not normalized, and different systems may carry different numbers of solutions. This is a *profound* difference from the standard theory. Adding up the individual multiplicities defines the total multiplicity, W^{tot}, as indicated in Fig. 10. With the correct normalization by W^{tot}, the multiplicity can be converted to a probability distribution.

Our emphasis on modeling individual, quantized events is largely what separates our concept from the Born rule or from the spectral function of G [5]. We calculate individually normalized events instead of the probability *of* a normalized event. In our theory, properties of the ensemble are built up from a distribution of individual events based on the bare particle degrees of freedom, just as they are in experiment.

In our picture, the wave function is not a probability amplitude [5]. Instead, we use an explicit model for collapse. The wave function is a carrier of information about fully quantized correlations between field operators. It has little quantitative meaning outside the context of our inverse problem.

An alternative approach to recovering the norm lost to virtual excitations could be to trace over all possible K, K' excitations to define a reduced correlation function in the single-particle subspace. Simply adding up all the different spectral layers would be somewhat analogous to the definition of the reduced single-particle density matrix [4]. In general, traces are performed when an observer only has access to a subspace of a system. We have demonstrated, however, that a trace is not the only option to treat inaccessible degrees of freedom. Our method adds contributions from

inaccessible degrees of freedom, like a trace, but combined so that their weighted sum creates a signal that matches the observation in the accessible subspace.

Our interpretation holds great promise for new physics. Again, the foundational structure of our concept is different than current theory. If only quantized solutions contribute to statistical mechanics of observables, there is a new entropic force based on counting quantized solutions. It is also possible that no quantized solutions exist. There is a new quantity, W^{tot}, to interpret. We have a complete phenomenology built around the concept that observable dynamics are described by collapse along the multiplicity surface that we will discuss in future work. A major component of this extended phenomenology is an internal spacetime that connects the two points of the collapse with the purpose of holding the information gained from the reduction of the probabilistic state. It dilates and contracts in order to hold the information gained from each event. We also consider the connections of the internal spacetime and entropic force to the geometry of the multiplicity surface through statistical mechanics. This discussion is reserved for a future manuscript.

8 Conclusion

The initial motivation for our study was the difference in size between the many-body state and the relatively small portion of it which can be measured. This is an unavoidable fact of the many-body problem and one which creates inconsistencies when jumping from the wave function to Green's function picture. To remedy this, we started our construction from the total Green's function, $\mathcal{G}$. At the endpoints of the correlation, we project all available degrees of freedom onto the observable degrees of freedom. Because of the reduction in dimensionality inherent to this process, there is freedom in choosing which pair of excitations to project into the observable subspace.

We argued that the relevant object in entangled systems is the entangled pair of particles. For this reason, our strategy is to quantize the creation, propagation, and annihilation of entangled pairs of particles instead of individual particles. We proposed that the observable event is a linear combination of spectral layers chosen so that the observed single-particle spectral function is quantized. This constraint fixes the projection freedom. When the system is measured, a quantized spectrum is projected onto the single-particle subspace. The measurement has a nonlocal effect on the system's past, consistent with quantum entanglement.

Regardless of fine details of the solution method, counting solutions that fix the freedom to the quantization constraint defines a multiplicity surface. The multiplicity includes both a combinatoric effect from solving our inverse problem and a purely numerical effect due to insensitivity of the quantized projection to small perturbations in the microscopic degrees of freedom. Knowledge of the multiplicity surface and the total multiplicity for all possible collapse events allows one to compute the probability of one collapse event occurring over another.

In practice, our numerical calculations nicely imitated the behavior of the spectral function of G for weakly-correlated systems. For strong correlation, however, we observe non-quasiparticle peaks in the multiplicity. These new peaks are the projection of virtual excitations into the single-particle subspace. Such non-quasiparticle peaks are not visible in the single-particle Green's function and a major difference from standard theory. We consider the description of such non-quasiparticle features a success of our approach.

This article is meant to encourage new ideas and more rigorous work to follow. There are many technical aspects that need to be considered in detail. A main goal of future work is to rigorously find signatures of entanglement in the projection matrix. Our focus in this work is on introducing new physical principles. Our concept could serve as a blueprint for a new quantum many-body theory.

This work was supported by the Academy of Finland through grant no. 316347.

Appendix: Projection via Löwdin Downfolding

We provide a final demonstration of the overcompleteness of time evolution through a subspace of the many-body Hamiltonian. The Löwdin downfolding method is well-known in condensed matter and quantum chemistry. We demonstrate it here to further show the robustness of our concept and refute a common belief in the Green's function community.

As shown in many references and applied many times [6–10], algebraic manipulations of the time independent Schrödinger equation give the energy-dependent subspace Hamiltonian

$$\mathcal{H}^{\text{eff}}(E) = P\mathcal{H}P + P\mathcal{H}Q\frac{1}{E - Q\mathcal{H}Q}Q\mathcal{H}P \tag{13}$$

for projection operators P and Q which can be taken to project onto the single-particle subspace of the Hamiltonian and all other configurations, respectively. Inserting this effective Hamiltonian into the Schrödinger propagator,

$$\overline{U}_{ij}(\omega) = \frac{1}{\omega - \mathcal{H}^{\text{eff}}(E)} \tag{14}$$

$$\overline{U}_{ij}(\omega) = \frac{1}{\omega - \left(P\mathcal{H}P + v\frac{1}{E - Q\mathcal{H}Q}v\right)} \,. \tag{15}$$

We see that the propagator now depends on *two* parameters with the dimension of energy: ω and E. The subspace has many more eigenstates than it could normally support, and many more than can be represented at any one time. The self-consistent selection of the eigenvalue E determines the eigenstate which is projected into the subspace. The subspace is overcomplete with information about the total system, just as when correlating all degrees of freedom in $\mathcal{G}$ and projecting onto $\overline{G}$. For the

Löwdin downfolding, E is a free parameter which represents the projection freedom analogous to K, K' in our projection matrix.

Downfolding the many-body Hamiltonian and inserting it into the propagator does *not* contribute a self-energy $\Sigma(\omega)$ to the propagating particle as in Dyson's equation. The effect of downfolding is to render the problem overcomplete and uncover the projection freedom we have already described. The Hamiltonian in the denominator of Eq. 15 is E-dependent, not ω-dependent.

Funding Open Access funding provided by Aalto University. This work was supported by the Academy of Finland through grant no. 316347.

Data Availability Data sharing not applicable to this article as no datasets were generated or analyzed during the current study.

References

1. Einstein, A., Podolsky, B., Rosen, N.: Can quantum-mechanical description of physical reality be considered complete? Phys. Rev. **47**, 777–780 (1935). https://doi.org/10.1103/PhysRev.47.777
2. Fetter, A.L., Walecka, J.D.: Quantum Theory of Many-particle Systems. Courier Dover Publications, Mineola, NY (1971)
3. Martin, R.M., Reining, L., Ceperley, D.M.: Interacting Electrons. Cambridge University Press, Cambridge (2016)
4. Helgaker, T., Jørgensen, P., Olsen, J.: Molecular Electronic-Structure Theory. Wiley, West Sussex (2014)
5. Born, M.: Quantenmechanik der stoßvorgänge. Z. Phys. **38**(11), 803–827 (1926)
6. Li Manni, G., Aquilante, F., Gagliardi, L.: Strong correlation treated via effective Hamiltonians and perturbation theory. J. Chem. Phys. **134**(3), 034114 (2011)
7. Dvorak, M., Rinke, P.: Dynamical configuration interaction: quantum embedding that combines wave functions and green's functions. Phys. Rev. B **99**, 115134 (2019)
8. Dvorak, M., Golze, D., Rinke, P.: Quantum embedding theory in the screened coulomb interaction: combining configuration interaction with GW/BSE. Phys. Rev. Mater. **3**, 070801 (2019)
9. Dzuba, V.A., Flambaum, V.V., Kozlov, M.G.: Combination of the many-body perturbation theory with the configuration-interaction method. Phys. Rev. A **54**, 3948–3959 (1996)
10. Li Manni, G., Ma, D., Aquilante, F., Olsen, J., Gagliardi, L.: Splitgas method for strong correlation and the challenging case of Cr_2. J. Chem. Theory Comput. **9**(8), 3375–3384 (2013)